SAND2007-5151C

LOW IMPEDANCE Z-PINCH DRIVERS WITHOUT POST-HOLE CONVOLUTE CURRENT ADDERS

David B. Seidel and Mark E. Savage
Sandia National Laboratories,* PO Box 5800, Albuquerque, NM 87185-1152 USA

Clifford W. Mendel, Jr.
Cove Consulting, Belle Haven, VA 23306 USA

Abstract

Present-day pulsed-power systems operating in the terawatt regime typically use current adders to operate at sufficiently low impedance. These adders necessarily involve magnetic nulls that connect the positive and negative electrodes. The resultant loss of magnetic insulation results in electron losses in the vicinity of the nulls that can severely limit the efficiency of the delivery of the system's energy to a load. In this paper, we describe an alternate transformer-based approach to obtaining low impedance. The transformer consists of coils whose windings are in parallel rather than in series, and does not suffer from the presence of magnetic nulls.

I. INTRODUCTION

Z-pinch radiation source drivers such as Z and ZR must supply very high currents at moderate (by pulsed power standards) voltage. This in turn requires very low inductance feeds. Presently this is accomplished by adding several higher impedance drivers in parallel using a post-hole convolute current adder. Unfortunately, current addition results in localized magnetic nulls that extend from the cathode to the anode [1]. Since the cathode surfaces emit electrons at the space-charge limit, the nulls result in electron losses. These losses are in addition to those due to magnetically insulated flow over most of the transmission lines, and, more importantly, these losses occur over small areas of the anode resulting in electrode damage and conducting gases that cause major current losses and further damage.

It is possible to replace the current adder (convolute) with a transformer that allows driver power to be combined in series with voltage adders, and then converted to lower voltage and higher current in the transformer. In contrast to common transformers, this transformer consists of coils whose windings are in parallel rather than series. These coils are similar to coils found in a number of other pulsed power devices, such as some ion diodes and triggered plasma opening switches.

There are several potential benefits to using an auto-transformer approach. Such a system would have no magnetic nulls to cause localized current losses. Moreover, the current multiplication ratio can easily be varied, resulting in a more versatile driver. There are also potential benefits in the way pulsed radiation source (PRS) wire loads would be installed that should increase the shot rate. The critical issues that must be addressed are achieving sufficient coupling between the primary and secondary circuits, and building a primary coil with adequate mechanical strength. This paper will describe the design of such a system, and will present preliminary results analyzing the performance of such a system in comparison to the standard post-hole convolute approach.

II. TRANSFORMER MODELING

Fig. 1 shows a radial plane cutaway view of a simple transformer. One-half of a primary coil and one-quarter of

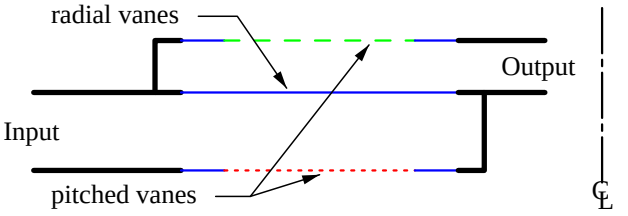

Figure 1. Simple transformer in cylindrical coordinates.

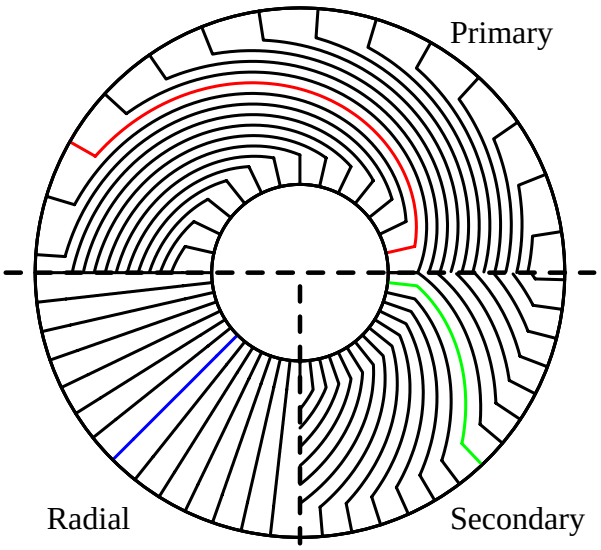

Figure 2. Composite r-θ view of transformer coils.

a secondary coil are shown in a composite drawing in Fig. 2. To give some idea of the angle subtended by the vanes, single primary and secondary vanes are shown in red and green, respectively. The lower-left quadrant of Fig. 2 also shows the radial vanes, of which one is shown in blue. In the simple transformer the two coils could be pitched in the same direction, or opposite directions as shown. The center conductor between the two coils consists of radial vanes (shown in blue in Fig. 1). Radial vanes allow the r,z components of the magnetic field to penetrate. The primary and secondary circuits could be attached as shown, or could be separated with separate radial vane sections, or could consist entirely of pitched conducting sections.

A somewhat more complicated system (see Fig. 3) would use an auto-transformer, in which a portion of the primary and secondary circuits are shared. By using an auto-transformer design, the wrap angle of the primary coils can be reduced (for the same current multiplication) which makes the coils more robust. Moreover, the primary and secondary coils are closer together which increases the coupling efficiency, $\eta = M^2 / L_p L_s$, where L_p and L_s are the self inductances of the primary and secondary coil, respectively, and M is the mutual inductance between them. Since azimuthal current due to the driver should run in the same azimuthal direction in the primary and secondary coils, whereas the radial current runs in opposite directions, the wrap of these two coils must be in the opposite direction.

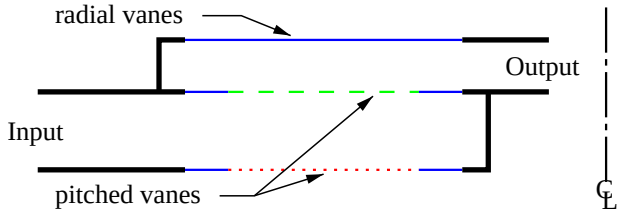

Figure 3. Auto-transformer in cylindrical coordinates.

Fig. 4 shows a double-sided auto-transformer. This design reduces the wrap angle of any individual coil, and increases the coupling efficiency. To insure that the azimuthal current in all four coils flows in the same direction, the sign of the wrap angles should alternate for each of the stacked coils.

A. Calculation of Self and Mutual Inductance

It is easy to show that for a given coil configuration, and any geometrically similar configuration, the coil's inductance L can be expressed in terms of a normalized inductance $\mathcal{L}$, i.e., $L = \mathcal{L}\delta\Delta\theta^2$, where $\Delta\theta$ is the total angle subtended by the vanes of the coil and δ is a scaling parameter for similar coils, i.e., coils that change in size, but not in shape. A coil's configuration includes its location, pitch figure, and any surrounding flux-excluding structure, which all need to be scaled in proportion to δ. We have chosen to define δ as the difference between the inner and outer radii of the spiral sections of the coils.

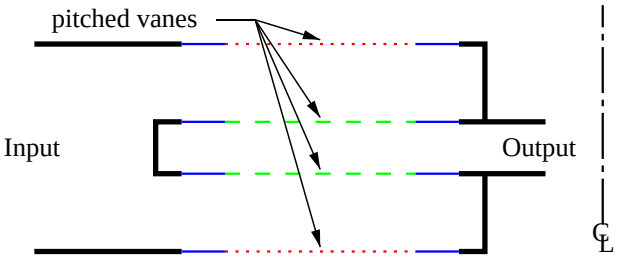

Figure 4. Double-sided auto-transformer in cylindrical coordinates.

The figure of the coil, i.e., the variation of the current pitch along the radial extent, can vary with radius and is defined to be $f(\rho)$, where $\rho = r/\delta$ and $\int_0^1 f(\rho)d\rho = 1$. The coil's pitch is defined as $P(r) \equiv r(\partial\theta/\partial r) = \Delta\theta\rho f(\rho)$. Note that two coils are geometrically similar only if their figures are the same. We have chosen to limit ourselves to $f(\rho) = 1$ for now. This figure spreads the magnetic pressures on the coils uniformly while storing much of the magnetic energy near the load.

Applying a similar process for two coils, p and s, in close proximity, and with the same δ, their mutual inductance M can be expressed in terms of a normalized mutual inductance $\mathcal{M}$, i.e., $M = \mathcal{M}\delta\Delta\theta_p\Delta\theta_s$. The coupling efficiency between the coils is then $\eta = \mathcal{M}^2 / \mathcal{L}^2$ and depends only upon the shape of the entire device, but not the scale size. The static magnetic code Atheta [2] was used to obtain values for $\mathcal{L}$ and $\mathcal{M}$. The geometry of the calculation is shown in Fig. 5.

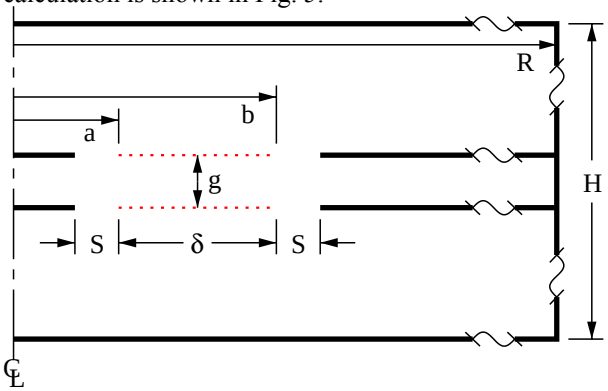

Figure 5. Geometry for Atheta inductance calculations. Note that R and H are not shown to scale.

The Atheta calculations were done in a large bounding box (large R and H) so that the values calculated can be considered to be for free-space coils. In the actual calculations only one half of the figure shown in Fig.5 needed to be done. Using $B_z = 0$ as a boundary condition on the center plane, the net normalized circuit inductance $2(\mathcal{L}\text{-}\mathcal{M})$ is measured. Using $B_r = 0$ yields the net normalized inductance for an open output, $2(\mathcal{M}+\mathcal{L})$. From these the values of $\mathcal{L}$ and $\mathcal{M}$ can be calculated. Fig. 6

shows the coupling efficiency η for several values of b/a (see Fig. 5) as a function of the normalized gap g/δ.

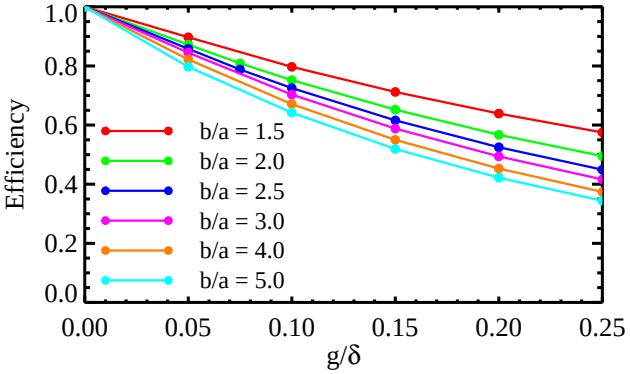

Figure 6. Transformer efficiency as a function of g for several ratios of outer to inner radius.

In a realizable system, the coils will connect to short sections of radial conductors, which will in turn connect to solid conductors which are needed to provide their support. The latter will exclude flux, and will reduce both inductance and mutual inductance. This is shown in Fig. 7, where the normalized self and mutual inductances are shown as a function of the spacing between the coils and the flux-excluding structure for b/a = 2 and g/δ = 0.075. Also shown is the corresponding coupling efficiency.

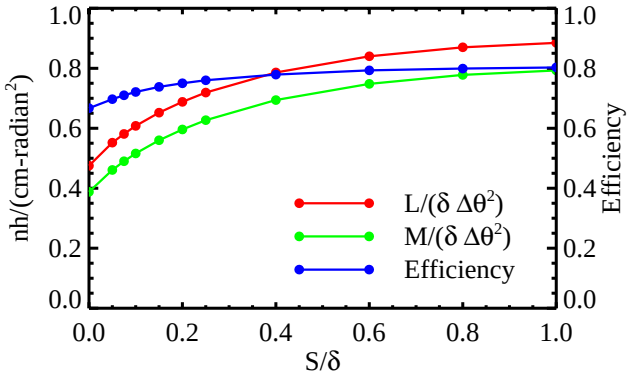

Figure 7. $\mathcal{L}$, $\mathcal{M}$, and η as a function of coil standoff S.

These data were encouraging, as the coupling efficiency and the inductances appeared to be reasonable for the devices we had in mind. While studying these data the idea of a double-sided auto-transformer occurred to us. The double-sided design (Fig. 4) has several advantages over the single-sided design of Fig. 3. Since the coil wrap angles need to be about half that of a single-sided design for the same inductance, the coils are stronger, or alternately, the inductance can be increased without increasing the wrap angle. Moreover, the coupling efficiencies are higher.

Atheta was use to compute $\mathcal{L}$ and $\mathcal{M}$ for a double-sided transformer, using the geometry shown in Fig. 8. Note that here we define $\Delta\theta_p$ and $\Delta\theta_s$ to be the wrap angle for single primary and secondary coils, respectively. Fig. 9 shows the coupling efficiency versus the normalized primary gap, g_p/δ, between a primary and secondary coils. The values of b/a = 2.0 and S/δ = 0.25 are the values we tentatively have chosen for study. We believe g_p/δ = 0.075 is reasonable. Three ratios of primary to secondary gap are shown, but the efficiency is insensitive to the ratio. The efficiency for the corresponding single-sided transformer is also shown. The improvement of the double-sided design over the single-sided design is appreciable, since the difference between the efficiency and one should be kept low.

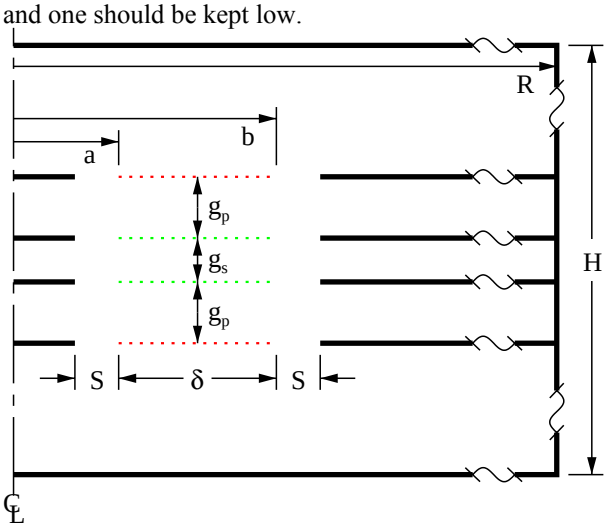

Figure 8. Geometry for Atheta inductance calculations of double-sided transformer.

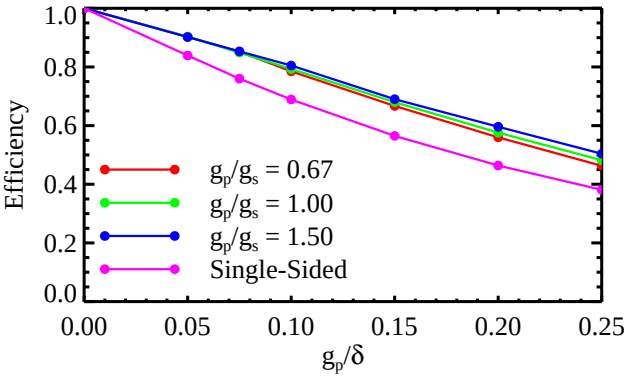

Figure 9. Double-sided transformer efficiency as a function of g_p for various ratios of primary to secondary gap. Single-sided efficiency is shown for comparison.

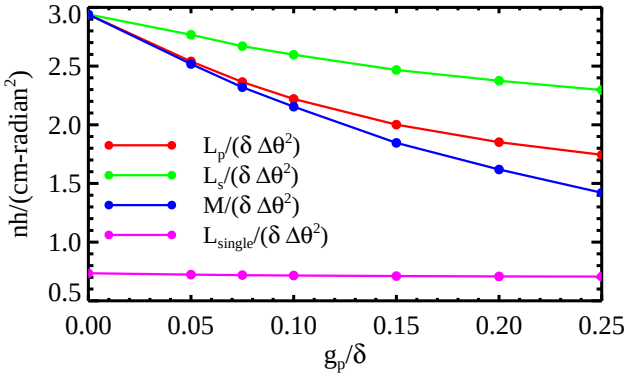

Figure 10. $\mathcal{L}_p$, $\mathcal{L}_s$, and $\mathcal{M}$ as a function of primary gap g_p.

Fig. 10 shows the normalized primary, secondary, and mutual inductances for $g_p/g_s = 1.5$. As the gaps go to zero, these should all approach four times that of a single coil (shown at the bottom), as they do. This is because the wrap has effectively been doubled.

B. Circuit Model for the Auto-Transformer System with a PRS Load

The simplest model for an auto-transformer-driven inductive load is shown in Fig. 11. With this circuit it is convenient to look at the inductance as seen by the source driver. We will call this inductance L_{eff}, given by

$$L_{eff} = L_0 + L_1(1-\eta) + (M+L_2)^2 L(s)/L_2[L_2 + L(s)]$$

where s is a distance parameter such as the radius in the case of a cylindrical pinch. The circuit equations are then $d(L_{eff} I)/dt = 2V_0(t) - Z_0 I$, where $V_0(t)$ and Z_0 describe the driver, and $F = (I^2/2)dL_{eff}/ds$, where F is the force on the load mass.

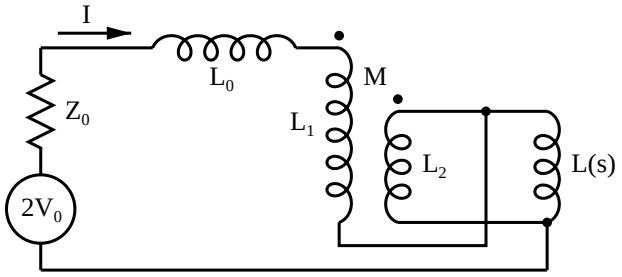

Figure 11. Circuit for auto-transformer system.

It is easily shown that it is desirable to make the change in L_{eff} as high as possible compared to the final value. For this reason, η should be close to one. It can also be shown that it is desirable to get the energy out of the driver and into magnetic energy before L_{eff} can expand appreciably. This is one of the advantages of a PRS load, since dL_{eff}/ds begins with a low value, and rises sharply at the end of the implosion.

However, there is the additional feature that the driver sees very low initial impedance, and very high late impedance. This reduces the efficiency somewhat due to reflected energy. With the auto-transformer system it may be possible to mitigate this effect somewhat because the current multiplication decreases and the voltage multiplication (always less than one) increases as the load inductance rises. The current multiplication at zero load inductance is given by

$$(M+L_2)/L_2 = \sqrt{\eta}\,\Delta\theta_p/\Delta\theta_s + 1 \equiv \sqrt{\eta}R_{wrap} + 1 .$$

The current multiplication in general is then

$$(M+L_2)/[L_2 + L(s)] = (\sqrt{\eta}R_{wrap} + 1)L_2/[L_2 + L(s)] .$$

1) PRS Load Model

For the PRS load we assume a cylindrical mass, m, of given height, h, and initial radius $r(0)$. The return current is at radius r_o. In addition we assume a light internal monatomic gas load of negligible mass. This gas load is heated by a very small (~3 mΩ) series resistance, Z_i, and by the adiabatic compression as the mass shell implodes. For a given load, the series resistance is adjusted using a circuit model of the Z machine convolute driver, so that the maximum internal energy in the gas load, and also the minimum radius, occur at the time of the X-ray peak for the appropriate Z experimental shot. This same load is then used in an auto-transformer model. The circuit for this model is same as the circuit shown in Fig 11, except for the addition of Z_i in series with the load inductance $L(s)$. Because of this addition, L_{eff} is no longer strictly valid, since the circuit equation now requires two coupled equations. However, because Z_i is so small, general characteristics derived from L_{eff} are reasonably accurate.

2) PRS model for the convolute (current adder) driver

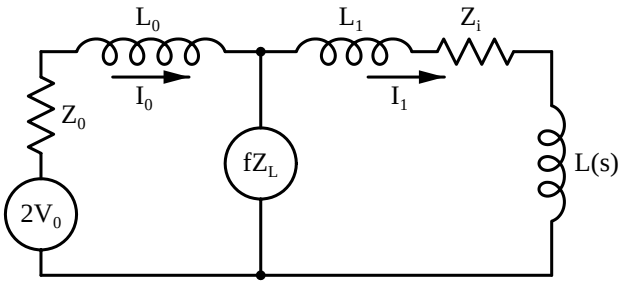

Figure 12. Circuit for convolute driver system.

This model (see Fig. 12) is the same as Struve's model [3] used to analyze Z PRS data, except for two changes. One is the use of the PRS model discussed above; the other is in the modeling of the current loss at the convolute. Struve used a constant $Z_{loss} = V_1/(I_o^2 - I^2)^{1/2}$ model, where Z_{loss} was set below the electron loss value to compensate for closure at the nulls due to material from the anode. We used a time dependent Z_{loss}. It began at the electron-loss-only value calculated by Pointon [4] for the Z convolute (0.4 Ω). When the energy deposition in the anode at the convolute reached an assigned threshold, we let the value of Z_{loss} decay exponentially with an assigned time constant. The threshold (25 kJ) and the time constant (50 ns) were set using the ICES data studied by Lemke [5]. These data had more accurate downstream current data than have been available in the more severe conditions near a Z pinch.

3) Parameters of an auto-transformer system powered by a Z-like driver

Assuming a 4 level system added in series rather than in parallel, we use V_0= 4×3.0=12 MV, and Z_0=4^2×0.12= 1.92Ω. Because of the characteristics of magnetically insulated flow, and also because desorbed gas and plasma closure rates tend to be independent of voltage, the impedance of the MITL can be much lower than four times that of the Z MITLs. However, the inductance near the insulator stack will be something like four times that of one of the Z levels. Our best estimate for L_0 is 50 nH.

Using the Atheta data, reasonable transformer parameters were chosen to be (see Fig. 8): a=20 cm, b=40 cm, g_p=1.5 cm, g_s=1.0 cm, $\Delta\theta_p$=2.4 radians (×2), $\Delta\theta_s$=0.7 radians (×2). From this, and including inductance from B_θ, L_1 = 331 nH, L_2 = 28 nH, M = 84 nH, η = 0.76. This adds the constant amount $(L_1\text{-}M^2/L_2) = L_1(1\text{-}\eta)$ = 79 nH to L_0.

4) Auto-transformer/convolute comparisons for a Z-like driver

We have written solvers for the two models using the commercial IDL software, complemented by the PFIDL data analysis tools [6]. Both models use the same driver and load as outlined above. This comparison is preliminary at the moment. The caveats include

- The transformer model has not been optimized,
- The load parameters have not been re-optimized for the transformer,
- There are no electron losses in the transformer model at present.

The first two items presumably cause the transformer modeling to under-perform, but the third definitely neglects losses that will occur. Although one or more Z_{loss} components are likely to be suitable, we do not yet have a way of setting the values. This has just begun to be studied using electromagnetic particle-in-cell modeling, as discussed in Section C. Fig. 13 shows the currents at the load and the internal energy of the load plotted versus time for both systems.

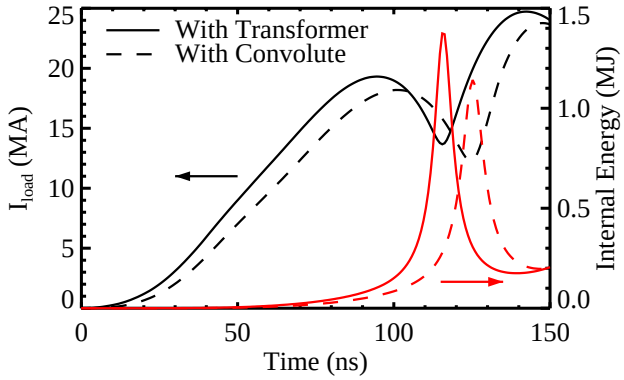

Figure 13. Comparison of load current and internal energy between transformer and convolute systems.

C. Electromagnetic Modeling

The transformer coils are three-dimensional objects as they are only invariant to rotations of multiples of $2\pi/N$ where N is the number of vanes in the coil. However, if N is very high (we expect to use 40 and 100 vane coils) these coils can be modeled as two-dimensional objects, as if N were infinite. There is an added component to L_1 and L_2 due to the finite number of vanes which can easily be calculated. It appears that this contribution to L_2 (~1 nH) should be included, but the contribution to L_1 can be neglected.

Although there is a coordinate system for which the individual coil vanes conform to coordinate lines, we do not have a code using coordinate systems other than Cartesian, cylindrical, or spherical coordinates. However, the 2D/3D electromagnetic, particle-in-cell simulation code Quicksilver [2] can model coils with an infinite number of vanes by using a tensor conductivity model in the plane of the coils.

Using Quicksilver (in fields-only mode) the inductances and mutual inductances agree with Atheta calculations within about 1% when the latter are corrected to include inductance due to azimuthal magnetic fields. The calculations included the coils, radial feed portions, solid conductors, and both used the same size bounding boxes. Figs. 14 and 15 show contours of stream function in the r,z plane for short-circuit and open-circuit cases, respectively.

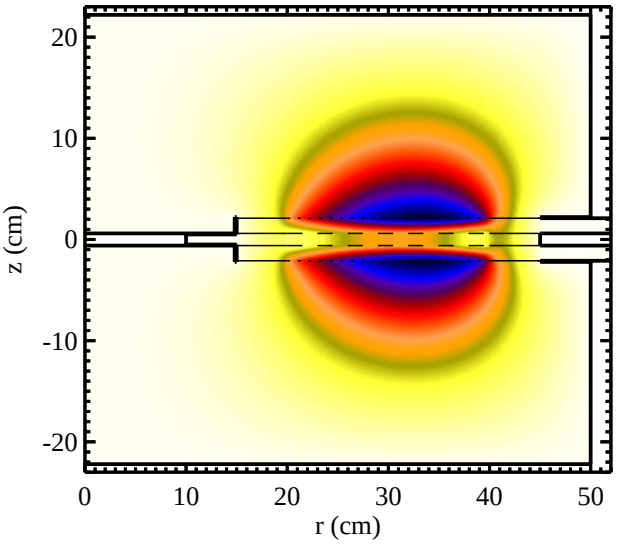

Figure 14. Stream function from Quicksilver simulation of a double-sided transformer with a short-circuit load located at r = 10 cm.

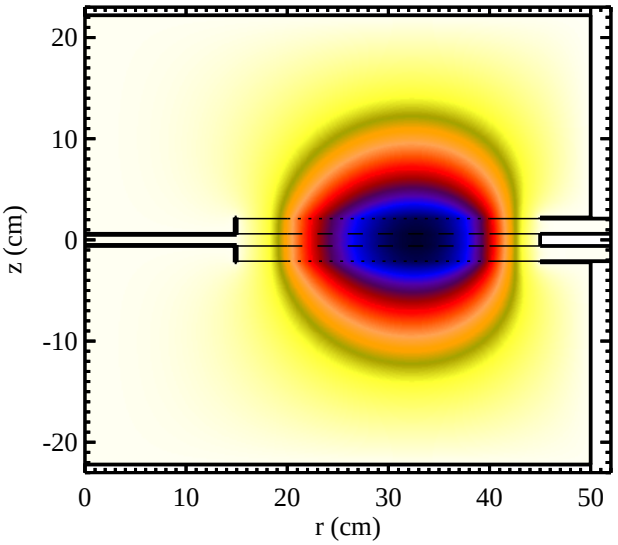

Figure 15. Stream function from Quicksilver simulation of a double-sided transformer with a open-circuit load.

Adding electron flow adds some modeling issues, namely space-charge-limited emission from coils and

electron capture by coils. Although we can run these calculations assuming these phenomena occur at solid surfaces, they presumably overstate the losses. We believe we can use some specialized simulations to study these effects, but have not yet begun such studies.

Initial simulations using the assumption of solid-surface emission and collection do show appreciable losses. This is to be expected when one considers the fact that field lines go directly across between the conductors at the coil input (see Figs. 14 and 15). Magnetically insulated electrons from the primary coil feeds cannot cross so much magnetic flux, and as electron charge builds up they can drift to the anode.

Although the currents are appreciable in these circumstances, these electron losses are spread uniformly in azimuth and over a sufficient radial extent that desorbed gas loads may be small. Moreover we are confident that these electron losses can be reduced appreciably with improved design.

III. Transformer Survivability

There are two possible damage mechanisms that need to be considered. The first is due to the magnetic pressure pushing transformer coils apart between the start of the power pulse and the time of maximum implosion (Fig. 14). Because the coils are five to six orders of magnitude heavier than the load and the pressures are lower than those on the load, the coils will not move much during this time period. The impulse on the coils can easily be calculated, and this can be used to get the net energy deposition. The answer amounts to only a few Joules, which is not significant.

The other possible problem would occur late in time, when current could remain in the MITLs due to insulator flash. The vertical magnetic fields (see Fig. 15) will try to squeeze the vanes together midway between their inner and outer radii. This has been seen in experiments with fast field coils made with very thin vanes. We have not yet made any calculation of this effect.

We do intend to make the coils robust. Moreover we believe we may be able to avoid insulator flash. In Z experiments, the collapse of the impedance across the convolute traps a large amount of magnetic flux in a rather small inductance. Because of this the system attempts to make an appreciable voltage reversal on the insulator. In the auto-transformer case, the inductance inside the insulator should go to $L_0 + L_1 + L_2 + 2M$ (577 nH for system modeled here), driving a much lower power pulse back into the driver's water section.

IV. SUMMARY

Our initial exploration of using parallel-winding transformers for high-current pulsed-power applications has been encouraging. We have demonstrated that transformers can have acceptable coupling efficiencies in realistic configurations. This is particularly true for double-sided auto-transformer systems. Initial investigation of the mechanical loads on the transformer coils in environments comparable to Sandia's Z-machine, although still preliminary, show no significant issues.

Much remains to be done to demonstrate the utility of this technology. Toward that end, we are continuing to study the issues associated with these devices. Probably the most important issue is the electron flow in the vicinity of the transformer coils, so we will continue our analysis and modeling in that area. We also need to improve our analysis of mechanical issues, particularly those occurring later in time with the possibility of insulator flash.

We are presently in the planning stages for a series of experiments, to be conducted on a relatively small pulsed-power driver, where we will refine our design and analyze its performance. If these experiments are successful, we hope to move them to an environment more like that of the Z-machine.

V. REFERENCES

[1] C. W. Mendel, Jr., T. D. Pointon, M. E. Savage, D. B. Seidel, I. Magne, and R. Vézinet, "Losses at magnetic nulls in pulsed-power transmission line systems," Physics of Plasmas, vol. 13, 043105, 2006.

[2] J. P. Quintenz, D. B. Seidel, M. L. Kiefer, T. D. Pointon, R. S. Coats, S. E. Rosenthal, T. A.. Mehlhorn, M. P. Desjarlais, and N. A. Krall, "Simulation Codes for Light-Ion Diode Modeling," Laser Part. Beams, vol. 12, pp. 283-324, 1994.

[3] K. Struve, private communication.

[4] T. Pointon, private communication.

[5] R. W. Lemke, M. D. Knudson, J-P. Davis, D. E. Bliss, and H. C. Harjes, "Self Consistent, 2D Magneto-Hydrodynamic Simulations of Magnetically Driven Flyer Plate Experiments on the Z-Machine," in Shock Compression of Condensed Matter – 2003, M. D. Furnish, Y. M. Gupta, and J. W. Forbes, Ed., American Inst. Phys. 0-7354-0180-0/04, Melville, NY, pp. 1175-1180.

[6] L. P. Mix, R. S. Coats, and D. B. Seidel, "PFIDL: Procedures for the Analysis and Visualization of Data Arrays," Tri-Laboratory Engineering Conference on Computational Modeling, Pleasanton, CA, Oct. 31-Nov. 2, 1995.